EUROPEAN JOURNAL OF PURE AND APPLIED MATHEMATICS
2025, Vol. 18, Issue 2, Article Number 5933
ISSN 1307-5543 – ejpam.com
Published by New York Business Global

Mathematical SEIR Model of the Lumpy Skin Disease Using Caputo-Fabrizio Fractional-Order

Rajagopalan Ramaswamy[1,*], Gunaseelan Mani[2], Radhakrishnan Mohanraj[3,4], Ozgur Ege[5]

[1] *Department of Mathematics, College of Science and Humanities in Alkharj, Prince Sattam Bin Abdulaziz University, Alkharj 11942, Saudi Arabia*
[2] *Department of Mathematics, Saveetha School of Engineering, Saveetha Institute of Medical and Technical Sciences, Chennai 602105, India*
[3] *Directorate of Learning and Development, SRM Institute of Science and Technology, Kattankulathur, Chennai, 603203, Tamil Nadu, India*
[4] *Department of Mathematics, SRM Institute of Science and Technology, Kattankulathur, Chennai, 603203, Tamil Nadu, India*
[5] *Department of Mathematics, Ege University, Bornova, Izmir, 35100, Turkey*

Abstract. UN SD Goal-3 focuses on good health and well-being, while the 15th goal focuses on life on land. This research aims to study an integral model of Lumpy Skin Disease to establish better knowledge of this condition. In this study, a Caputo-Fabrizio fractional-order model for the dynamics of Lumpy Skin Disease (LSD) is analysed. Using the Picard-Lindelöf theorem in the Banach space $\mathcal{C}([0,1],\mathbb{R})$ with the supremum norm $\|\phi\| = \max_{\mathtt{s}\in[0,1]} |\phi(\mathtt{s})|$, we prove existence and uniqueness of solutions via fixed-point theory. The positivity, boundedness, and Ulam-Hyers stability of the model are established. Disease-free and endemic equilibria are derived, the basic reproduction number $\mathcal{R}_0$ is computed, and sensitivity analysis is conducted to identify critical transmission parameters. A novel Newton interpolation-based numerical scheme is developed and compared with finite difference method, with superior convergence rates being demonstrated. How non-integer operators enhance LSD progression modeling compared to classical approaches is revealed by fractional-order simulations. Actionable insights for disease control are provided by our results while the efficacy of Caputo-Fabrizio derivatives in epidemiological modeling is demonstrated which will help in framing policies to have a healthy society, SDG-3 and other related goals of UN.

2020 Mathematics Subject Classifications: 65L60, 41A10, 35N70, 65L20

Key Words and Phrases: Fixed point theory, Caputo-Fabrizio, Ulam-Hyers stability

*Corresponding author.
DOI: https://doi.org/10.29020/nybg.ejpam.v18i2.5933

Email addresses: r.gopalan@psau.edu.sa (R Ramaswamy), mathsguna@yahoo.com (G.Mani), radhakrm@srmist.edu.in (R.Mohanraj), ozgur.ege@ege.edu.tr (O.Ege)

1. Introduction

The United nations [1] has set seventeen goals for sustaintable development (SDG) and SDG-3 is related to Health while SDG-15 is focussed on Life on Land. Living beings on earth are prone to infections and one such disease is Lumpy Skin Disease (LSD), that exists as an infection caused by the Lumpy Skin Disease Virus (LSDV) which possesses 150 kb of double-stranded DNA. The virus belongs to Capripoxvirus genera within the Chordopoxviridae subfamily of Poxviridae family [2, 3]. The genus Capripoxvirus comprises three confirmed viral members: Goatpox Virus (GTPV) and Sheeppox Virus (SPPV) alongside Lumpy Skin Disease Virus (LSDV). Electron microscope images show LSDV exhibits morphological patterns shared by other Poxviridae viruses similar to the vaccinia virus [4]. The virus has limited host range due to its restriction of transmission to two main hosts including cattle (Bos indicus or Bos taurus) and domestic water buffaloes (Bubalus bubalis) [5–7]. The Range Management Pathogens Research Unit in Georgia has studied how LSDV affects wild mammals including giraffes and camels as well as wildebeests [8–10].

Active transmission of disease occurs when animals transmit the virus through skin contact with lesions and milk and through the bloodfeeding activities of biting flies and mosquitoes and ticks [11–14]. The disease transmission rate is greater for these seasons because insect vectors are both more numerous and active [15]. Skilled shedding by the virus happens through nasal discharge along with skin lesions and saliva as well as lachrymal secretions to transmit disease from ill to well animals [12, 16].

An outbreak of LSD originated in India during 2019 followed by multiple serious occurrences. The newest spell of LSD outbreak started during May 2022 and extensively damaged 15 Indian states that led to about 100,000 cattle fatalities and considerable economic loss [17]. Within India's highly important livestock production industry LSD leads to animal mortality along with milk yield declines while creating additional economic impacts through movement limitations [17]. Under India's 308 million cattle population the prevention and control of infectious diseases including LSD stands as a vital necessity [18]. Comparable changes occur within diseased animals because of LSD resulting in mastitis along with necrotic hepatitis and lymphadenitis and orchitis and myocardial damage [19].

WHO has established LSD as an eligible disease for notification according to[20]. Surveillance confirmed the first documented case of LSD in Zambia in 1931 but the disease stayed within Sub-Saharan Africa until 1989 when it expanded into the Middle East and Asia [21–23]. Initial identification of LSDV occurred in Russia when the disease appeared in Southeast Europe in 2016 followed by its discovery in India and several neighboring Asian countries such as China and Nepal Thailand and Bangladesh plus Bhutan in November 2019 [24, 25]. From 2019 onward LSD spread rapidly to impact more than two million cattle during 2022. The symptoms typically occur within 1-4 weeks after a patient contracts the infection and high fever joins nasal or eye drainage along with appetite loss and nodular skin breakouts [26]. Public deaths from LSD have been reported between 5-45% during outbreaks in Rajasthan, Gujarat, Uttar Pradesh, and Punjab, Haryana, Karnataka along with West Bengal and Maharashtra [27–29].

Indian authorities have built a series of initiatives aimed at stopping animal disease spread which include massive vaccination programs combined with animal sequestration areas and restrictions on animal movement. Early detection remains difficult together with limited staff knowledge about disease spread across affected zones. Since its emergence from prior poxvirus species, LSDV expanded its network of hosts and harm potential through double-stranded DNA virus homologous recombination processes [30]. Through genome sequencing the study team identified current LSDV genetic variants that existed in India. Phylogenetic examination established two distinguishable variant classes having important variations in their mutation (SNP) pattern. Yasir et al. [31] studied the competition model in fractional derivatives of Caputo Fabrizio type through implementation of Newton based polynomials. Singh et al. [32] studied the fractional-order compartmental model for cervical cancer. HPV serves as the cause for cervical cancer to develop. This worldwide phenomenon receives attention through the utilization of the Caputo-Fabrizio fractional operator that contains antiretroviral medication treatment sections. Kumari et al. [33] established a mathematical model for coronavirus using the Caputo-Fabrizio fractional derivative.

The diabetes model and its complications were examined by Singh et al. [34] using Caputo-Fabrizio fractional derivatives. A new model of Rabies disease analysis conducted by Aydogan et al. [35] utilized Caputo-Fabrizio fractional derivatives. Butt [36] proposed a new fractional model of LSD dynamics which utilized the Atangana Baleanu fractional derivative to model disease transmission patterns and disease memory effects.

To develop a model for Lumpy Skin Disease (LSD), the total population $\mathcal{N}(\mathsf{s})$ is categorized into four distinct compartments: The population contains four subsections including susceptible $\mathcal{S}(\mathsf{s})$ exposed $\mathcal{E}(\mathsf{s})$ infected $\mathcal{I}(\mathsf{s})$ and recovered $\mathcal{R}(\mathsf{s})$. Therefore, at any given time t, the total population is expressed as:

$$\mathcal{N}(\mathsf{s}) = \mathcal{S}(\mathsf{s}) + \mathcal{E}(\mathsf{s}) + \mathcal{I}(\mathsf{s}) + \mathcal{R}(\mathsf{s}).$$

The susceptible class $\mathcal{S}(\mathsf{s})$ contains animals which can develop virus illnesses from contact with virus carriers. Exposed cattle arise through contacts between susceptible cattle and virus-infected cattle who advance to the exposed class $\mathcal{E}(\mathsf{s})$. Exposure indicates that cattle within this population have become infected but showcase no contagious characteristics at present.can become ill due to the interaction with the cattle carrying virus. When cattle from the susceptible class interact with the infections cattle become exposed cattle and hence move to the exposed class $\mathcal{E}(\mathsf{s})$. So, the exposed class is the class consisting of cattle that have become infected but not infectious till now. The following stage comes in the form of an infected set of cattle which the symbol $\mathcal{I}(\mathsf{s})$ defines. Any virus which establishes itself in exposed cattle creates infectious beings which transition from the exposed class $\mathcal{E}(\mathsf{s})$ to the infected class $\mathcal{I}(\mathsf{s})$. Pros of virus transmission exist whenever a cattle that is currently infectious becomes able to replicate and spread the virus. At the next stage exists the recovered class denoted as $\mathcal{R}(\mathsf{s})$. Higher levels of immunity exist in some cattle population leading them to recover from the disease more efficiently. Proper medication against infections allows these cattle to enter the recovered class. Such cattle types make up this category. All state variables $\mathcal{S}(\mathsf{s})$, $\mathcal{E}(\mathsf{s})$, $\mathcal{I}(\mathsf{s})$, $\mathcal{R}(\mathsf{s})$ meet the requirement of

continuous differentiability when considered over t in the time interval $[0, \infty)$. The flow pattern for LSD is shown in the Fig. 1 which in the form of nonlinear ordinary differential equations is given as:

$$\begin{aligned}
\frac{d\mathcal{S}}{d\mathsf{s}} &= \alpha\mathcal{N} - \beta\mathcal{S}\mathcal{I} + \theta\mathcal{R} - \phi\mathcal{S}, \\
\frac{d\mathcal{E}}{d\mathsf{s}} &= \beta\mathcal{S}\mathcal{I} - \gamma\mathcal{E} - \phi\mathcal{E}, \\
\frac{d\mathcal{I}}{d\mathsf{s}} &= \gamma\mathcal{E} - \omega\mathcal{I} - \phi\mathcal{I}, \\
\frac{d\mathcal{R}}{d\mathsf{s}} &= \omega\mathcal{I} - \theta\mathcal{R} - \phi\mathcal{R},
\end{aligned}$$

along with the following non-negative initial conditions.

$$\mathcal{S}(0) = \mathcal{S}_0, \mathcal{E}(0) = \mathcal{E}_0, \mathcal{I}(0) = \mathcal{I}_0, \mathcal{R}(0) = \mathcal{R}_0.$$

The rest of the paper is organised as follows: In Section 2 we present the LSD model

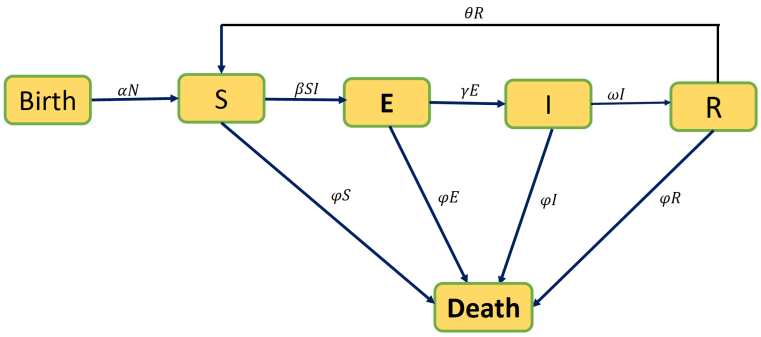

Figure 1: Flow chart

Table 1: Description of the parameters used in the model (1)

Parameter	Description	Values	Source
α	Birth rate	0.0114	[37]
β	Infection rate	0.00011412	[38]
γ	Progression rate from exposed to infected	0.95	[38]
ω	Recovery rate	0.14	Assumed
ϕ	Natural death rate	0.0057	Assumed
θ	Loss of immunity rate	0.007	Assumed

with $(\mathfrak{CF})$ derivative and review some model basic preliminaries and present and establish the results for positivity, boundedness, existence and uniqueness of the solutions for the model. In section-3 we analyyse the Ulam-Hyers stability and investigate the disease-free and disease-endemic equilibrium points in section-4. The numerical scheme is presented in Section-5 and the results are discussed in Section-6, which we believe will help in

formulating policies for restricting the spread of LSD and thus attain the SDG-3 as well as SDG-15 and other related goals of [1]. Finally we conclude the article with scope for further research.

2. Lumpy Skin Disease with Caputo-Fabrizio

The lumpy skin disease model with Caputo-Fabrizio($\mathfrak{CF}$) derivative is given by

$$\begin{cases} {}^{\mathfrak{CF}}\mathcal{D}_{\mathsf{s}}^{\mathsf{a}}\mathcal{S} &= \alpha\mathcal{N} - \beta\mathcal{S}\mathcal{I} + \theta\mathcal{R} - \phi\mathcal{S}, \\ {}^{\mathfrak{CF}}\mathcal{D}_{\mathsf{s}}^{\mathsf{a}}\mathcal{E} &= \beta\mathcal{S}\mathcal{I} - \gamma\mathcal{E} - \phi\mathcal{E}, \\ {}^{\mathfrak{CF}}\mathcal{D}_{\mathsf{s}}^{\mathsf{a}}\mathcal{I} &= \gamma\mathcal{E} - \omega\mathcal{I} - \phi\mathcal{I}, \\ {}^{\mathfrak{CF}}\mathcal{D}_{\mathsf{s}}^{\mathsf{a}}\mathcal{R} &= \omega\mathcal{I} - \theta\mathcal{R} - \phi\mathcal{R}, \end{cases} \tag{1}$$

with a being the fractional order $0 < \mathsf{a} < 1$ subject to the following initial conditions

$$\mathcal{S}(0) = \mathcal{S}_0, \mathcal{E}(0) = \mathcal{E}_0, \mathcal{I}(0) = \mathcal{I}_0, \mathcal{R}(0) = \mathcal{R}_0. \tag{2}$$

2.1. Model basic preliminaries

Here, we give some of the mathematical preliminaries in the form of theorems, which we shall apply to prove the positivity and uniqueness and positivity of lumpy skin disease model with Caputo-Fabrizio($\mathfrak{CF}$) (1) as defined [39, 40] respectively. More details, one can read [41–43]. We assume the space $\{\phi(\mathsf{s}) \in \mathcal{C}([0,1] \to \mathbb{R})\}$ with

$$||\phi|| = \max_{\mathsf{s}\in[0,1]} |\phi(\mathsf{s})|. \tag{3}$$

The definitions are stated as follows.

Definition 1. *Let $\phi : \mathbb{R}^+ \to \mathbb{R}$ and $\mathsf{a} \in (\mathfrak{n}-1, \mathfrak{n})$, $\mathfrak{n} \in \mathbb{N}$. The left Caputo fractional derivative of order a of the function ϕ is given by the following equality:*

$${}_0^{\mathcal{C}}\mathcal{D}_{\mathsf{s}}^{\mathsf{a}}(\phi(\mathsf{s})) = \frac{1}{\Gamma(\mathfrak{n}-\mathsf{a})}\int_0^{\mathsf{s}} (\mathsf{s}-\mathfrak{s})^{\mathfrak{n}-\mathsf{a}-1}\phi^{(\mathfrak{n})}(\mathfrak{s})d\mathfrak{s},\ \mathsf{s} > 0.$$

Definition 2. *The fractional integral associate to the new fractional integral with power-law kernel is defined as:*

$${}_0^{\mathcal{C}}\mathcal{I}_{\mathsf{s}}^{\mathsf{a}}(\phi(\mathsf{s})) = \frac{1}{\Gamma(\alpha)}\int_0^{\mathsf{s}} (\mathsf{s}-\mathfrak{s})^{\mathsf{a}-1}\phi(\tau)d\tau.$$

Definition 3. *Assume $\phi(\mathsf{s}) \in \mathcal{H}^1(\mathfrak{l}_1, \mathfrak{l}_2)$, for $\mathfrak{l}_2 > \mathfrak{l}_1$, $\tau \in [0,1]$. The $\mathfrak{CF}$ fractional operator is given as*

$${}^{\mathfrak{CF}}\mathcal{D}_{\mathsf{s}}^{\mathsf{a}}(\phi(\mathsf{s})) = \frac{\mathcal{M}(\mathsf{a})}{(1-\mathsf{a})}\int_{\mathfrak{l}_1}^{\mathfrak{l}_2} \phi'(\sigma)exp\bigg(-\mathsf{a}\frac{\mathsf{s}-\sigma}{1-\sigma}\bigg)d(\sigma),\ \ 0 < \mathsf{a} < 1,$$

$$= \frac{d\phi}{d\mathsf{s}}, \ \mathsf{a} = 1, \tag{4}$$

where $\mathcal{M}(\mathsf{a}) = 1 - \mathsf{a} + \dfrac{\mathsf{a}}{\Gamma(\mathsf{a})}$ *is a normalization function which satisfies the condition,* $\mathcal{M}(0) = \mathcal{M}(1) = 1$.

Definition 4. *The integral operator of fractional order corresponding to the* $\mathfrak{CF}$ *fractional derivative is stated as follows*

$$\begin{aligned}\mathcal{J}_{\mathsf{s}}^{\mathsf{a}}(\phi(\mathsf{s})) = &\frac{2(1-\mathsf{a})}{(2-\mathsf{a})\mathcal{M}(\mathsf{a})}\phi(\mathsf{s}) \\ &+ \frac{2\mathsf{a}}{(2-\mathsf{a})\mathcal{M}(\mathsf{a})}\int_0^{\mathsf{s}} \phi(\xi)d\xi, \ \ \mathsf{s} \geq 0.\end{aligned} \tag{5}$$

Definition 5. *The Laplace transform of* ${}^{\mathfrak{CF}}\mathcal{D}_{\mathsf{s}}^{\mathsf{a}}\phi(\mathsf{s})$ *is represented as follows*

$$\mathcal{L}[{}^{\mathfrak{CF}}\mathcal{D}_{\mathsf{s}}^{\mathsf{a}}\phi(\mathsf{s})] = \mathcal{M}(\mathsf{a})\frac{\kappa\mathcal{L}[-\phi(\mathsf{s})] - \phi(0)}{\kappa + \mathsf{a}(1-\kappa)}. \tag{6}$$

Theorem 1. *[44](Banach Contraction Theorem) Let* $(\mathcal{P}, \mathsf{d})$ *be a complete metric space, and let* $\mathsf{H} : \mathcal{P} \to \mathcal{P}$ *be a contraction on* $\mathcal{P}$*. Then* H *has a unique fixed point, say* $\mathsf{u} \in \mathcal{P}$*.*

2.2. Positivity of Solutions

Theorem 2. *For non-negative initial conditions* $\mathcal{S}(0), \mathcal{E}(0), \mathcal{I}(0), \mathcal{R}(0) \geq 0$*, the solutions of system* (1) *remain non-negative for all* $\mathsf{s} > 0$*.*

Proof. We employ the generalized mean value theorem for Caputo-Fabrizio derivatives:

$$\begin{cases} {}^{\mathfrak{CF}}\mathcal{D}_{\mathsf{s}}^{\mathsf{a}}\mathcal{S}\Big|_{\mathcal{S}=0} &= \alpha\mathcal{N} + \theta\mathcal{R} \geq 0, \\ {}^{\mathfrak{CF}}\mathcal{D}_{\mathsf{s}}^{\mathsf{a}}\mathcal{E}\Big|_{\mathcal{E}=0} &= \beta\mathcal{S}\mathcal{I} \geq 0, \\ {}^{\mathfrak{CF}}\mathcal{D}_{\mathsf{s}}^{\mathsf{a}}\mathcal{I}\Big|_{\mathcal{I}=0} &= \gamma\mathcal{E} \geq 0, \\ {}^{\mathfrak{CF}}\mathcal{D}_{\mathsf{s}}^{\mathsf{a}}\mathcal{R}\Big|_{\mathcal{R}=0} &= \omega\mathcal{I} \geq 0. \end{cases}$$

Since all derivatives are non-negative at the boundary of each compartment, the solutions remain non-negative for all $\mathsf{s} \geq 0$.

2.3. Boundedness of Solutions

Theorem 3 (Boundedness)**.** *The total population $\mathcal{N}(\mathsf{s})$ is bounded such that:*

$$\mathcal{N}(\mathsf{s}) \leq \max\left(\mathcal{N}(0), \frac{\alpha\mathcal{N}}{\phi}\right), \quad \forall \mathsf{s} \geq 0$$

Proof. From the system (1), the total population $\mathcal{N}(\mathsf{s})$ satisfies:

$$^{\mathfrak{CF}}\mathcal{D}^{\mathsf{a}}_{\mathsf{s}}\mathcal{N} = \alpha\mathcal{N} - \phi\mathcal{N} - \omega\mathcal{I}.$$

Since $-\omega\mathcal{I} \leq 0$, we have the inequality:

$$^{\mathfrak{CF}}\mathcal{D}^{\mathsf{a}}_{\mathsf{s}}\mathcal{N} \leq (\alpha - \phi)\mathcal{N}.$$

Using the Caputo-Fabrizio (CF) fractional derivative and its corresponding integral operator, the equivalent integral form is:

$$\mathcal{N}(\mathsf{s}) - \mathcal{N}(0) = \frac{2(1-\mathsf{a})}{(2-\mathsf{a})\mathcal{M}(\mathsf{a})}(\alpha - \phi)\mathcal{N} + \frac{2\mathsf{a}}{(2-\mathsf{a})\mathcal{M}(\mathsf{a})}\int_0^{\mathsf{s}}(\alpha - \phi)\mathcal{N}(\xi)d\xi.$$

Substituting $\mathcal{M}(\mathsf{a}) = 1 - \mathsf{a} + \frac{\mathsf{a}}{\Gamma(\mathsf{a})}$, this becomes:

$$\mathcal{N}(\mathsf{s}) - \mathcal{N}(0) = \frac{2(1-\mathsf{a})(\alpha - \phi)\mathcal{N}}{(2-\mathsf{a})\left(1 - \mathsf{a} + \frac{\mathsf{a}}{\Gamma(\mathsf{a})}\right)} + \frac{2\mathsf{a}(\alpha - \phi)}{(2-\mathsf{a})\left(1 - \mathsf{a} + \frac{\mathsf{a}}{\Gamma(\mathsf{a})}\right)}\int_0^{\mathsf{s}}\mathcal{N}(\xi)d\xi.$$

so the equation simplifies to:

$$\mathcal{N}(\mathsf{s}) - \mathcal{N}(0) = \kappa(\mathsf{a})(1-\mathsf{a})(\alpha - \phi)\mathcal{N} + \kappa(\mathsf{a})\mathsf{a}(\alpha - \phi)\int_0^{\mathsf{s}}\mathcal{N}(\xi)d\xi. \tag{7}$$

where,

$$\kappa(\mathsf{a}) = \frac{2}{(2-\mathsf{a})\left(1 - \mathsf{a} + \frac{\mathsf{a}}{\Gamma(\mathsf{a})}\right)},$$

Case 1: $\alpha \leq \phi$ **in** (7)

If $\alpha \leq \phi$, then $(\alpha - \phi) \leq 0$. The right-hand side of the inequality:

$$^{\mathfrak{CF}}\mathcal{D}^{\mathsf{a}}_{\mathsf{s}}\mathcal{N} \leq (\alpha - \phi)\mathcal{N}$$

is non-positive. Thus, $\mathcal{N}(\mathsf{s})$ cannot increase beyond its initial value:

$$\mathcal{N}(\mathsf{s}) \leq \mathcal{N}(0), \quad \forall \mathsf{s} \geq 0.$$

Case 2: $\alpha > \phi$ **in** (7)

If $\alpha > \phi$, then $(\alpha - \phi) > 0$. Rearrange the simplified equation:

$$\mathcal{N}(\mathsf{s}) - \mathcal{N}(0) = \kappa(\mathsf{a})(1-\mathsf{a})(\alpha-\phi)\mathcal{N} + \kappa(\mathsf{a})\mathsf{a}(\alpha-\phi)\int_0^{\mathsf{s}} \mathcal{N}(\xi)d\xi.$$

Let $\mathcal{U} = 1 - \kappa(\mathsf{a})(1-\mathsf{a})(\alpha-\phi)$, assuming $K > 0$ (valid for small enough a). Dividing through by K, we get:

$$\mathcal{N}(\mathsf{s}) \leq \frac{\mathcal{N}(0)}{\mathcal{U}} + \frac{\kappa(\mathsf{a})\mathsf{a}(\alpha-\phi)}{\mathcal{U}}\int_0^{\mathsf{s}} \mathcal{N}(\xi)d\xi.$$

Applying a Grönwall-type inequality, this yields:

$$\mathcal{N}(\mathsf{s}) \leq \mathcal{N}(0)\exp\left(\frac{\kappa(\mathsf{a})\mathsf{a}(\alpha-\phi)}{\mathcal{U}}\mathsf{s}\right).$$

As $\mathsf{s} \to \infty$, $\mathcal{N}(\mathsf{s})$ converges to a steady state determined by the balance between growth (α) and decay (ϕ):

$$\mathcal{N}(\mathsf{s}) \leq \max\left(\mathcal{N}(0), \frac{\alpha\mathcal{N}}{\phi}\right).$$

This completes the proof.

2.4. Existence and uniqueness of solutions of the $\mathfrak{CF}$ model

This section proves the existence and uniqueness of the solution to the proposed model (1) using fixed point theorem. To facilitate this analysis, model (1) can be expressed as follows:

$$\begin{cases} {}^{\mathfrak{CF}}\mathcal{D}_{\mathsf{s}}^{\mathsf{a}}\mathcal{S} &= \mathcal{K}_1(\mathsf{s},\mathcal{S}), \\ {}^{\mathfrak{CF}}\mathcal{D}_{\mathsf{s}}^{\mathsf{a}}\mathcal{E} &= \mathcal{K}_2(\mathsf{s},\mathcal{E}), \\ {}^{\mathfrak{CF}}\mathcal{D}_{\mathsf{s}}^{\mathsf{a}}\mathcal{I} &= \mathcal{K}_3(\mathsf{s},\mathcal{I}), \\ {}^{\mathfrak{CF}}\mathcal{D}_{\mathsf{s}}^{\mathsf{a}}\mathcal{R} &= \mathcal{K}_4(\mathsf{s},\mathcal{R}), \end{cases} \tag{8}$$

where

$$\begin{cases} \mathcal{K}_1(\mathsf{s},\mathcal{S}) &= \alpha\mathcal{N} - \beta\mathcal{S}\mathcal{I} + \theta\mathcal{R} - \phi\mathcal{S}, \\ \mathcal{K}_2(\mathsf{s},\mathcal{E}) &= \beta\mathcal{S}\mathcal{I} - \gamma\mathcal{E} - \phi\mathcal{E}, \\ \mathcal{K}_3(\mathsf{s},\mathcal{I}) &= \gamma\mathcal{E} - \omega\mathcal{I} - \phi\mathcal{I}, \\ \mathcal{K}_4(\mathsf{s},\mathcal{R}) &= \omega\mathcal{I} - \theta\mathcal{R} - \phi\mathcal{R}. \end{cases} \tag{9}$$

Applying fractional integral operator given in (5), system (8) reduces to the Volterra integral type of order $0 < \mathsf{a} < 1$ given by

$$\begin{cases} \mathcal{S}(\mathsf{s}) &= \mathcal{S}(0) + \frac{2(1-\mathsf{a})}{(2-\mathsf{a})\mathcal{M}(\mathsf{a})}\mathcal{K}_1(\mathsf{s},\mathcal{S}) + \frac{2\mathsf{a}}{(2-\mathsf{a})\mathcal{M}(\mathsf{a})}\int_0^{\mathsf{s}}\mathcal{K}_1(\xi,\mathcal{S})d\xi, \\ \mathcal{E}(\mathsf{s}) &= \mathcal{E}(0) + \frac{2(1-\mathsf{a})}{(2-\mathsf{a})\mathcal{M}(\mathsf{a})}\mathcal{K}_2(\mathsf{s},\mathcal{E}) + \frac{2\mathsf{a}}{(2-\mathsf{a})\mathcal{M}(\mathsf{a})}\int_0^{\mathsf{s}}\mathcal{K}_2(\xi,\mathcal{E})d\xi, \\ \mathcal{I}(\mathsf{s}) &= \mathcal{I}(0) + \frac{2(1-\mathsf{a})}{(2-\mathsf{a})\mathcal{M}(\mathsf{a})}\mathcal{K}_3(\mathsf{s},\mathcal{I}) + \frac{2\mathsf{a}}{(2-\mathsf{a})\mathcal{M}(\mathsf{a})}\int_0^{\mathsf{s}}\mathcal{K}_3(\xi,\mathcal{I})d\xi, \\ \mathcal{R}(\mathsf{s}) &= \mathcal{R}(0) + \frac{2(1-\mathsf{a})}{(2-\mathsf{a})\mathcal{M}(\mathsf{a})}\mathcal{K}_4(\mathsf{s},\mathcal{R}) + \frac{2(1-\mathsf{a})}{(2-\mathsf{a})\mathcal{M}(\mathsf{a})}\int_0^{\mathsf{s}}\mathcal{K}_4(\xi,\mathcal{R})d\xi. \end{cases} \tag{10}$$

($\mathcal{G}$:) For proving our results, we consider the following assumption: For this, $\mathcal{S}(\mathsf{s}), \mathcal{S}^\star(\mathsf{s}), \mathcal{E}(\mathsf{s}), \mathcal{E}^\star(\mathsf{s}), \mathcal{I}(\mathsf{s}), \mathcal{I}^\star(\mathsf{s}), \mathcal{R}(\mathsf{s}), \mathcal{R}^\star(\mathsf{s}) \in \mathcal{L}[0,1]$ be continuous such that $||\mathcal{S}(\mathsf{s})|| \leq \mathfrak{c}_1$, $||\mathcal{E}(\mathsf{s})|| \leq \mathfrak{c}_2$, $||\mathcal{I}(\mathsf{s})|| \leq \mathfrak{c}_3$ and $||\mathcal{R}(\mathsf{s})|| \leq \mathfrak{c}_4$, for some positive constants $\mathfrak{c}_1, \mathfrak{c}_2, \mathfrak{c}_3, \mathfrak{c}_4 > 0$.

Theorem 4. *Each kernel $(\mathcal{K}_1, \mathcal{K}_2, \mathcal{K}_3, \mathcal{K}_4)$ satisfy the Lipschitz condition under the assumption $(\mathcal{G})$ and*

$$\mathfrak{j}_\mathfrak{i} < 1, \text{ for } \mathfrak{i} = 1,2,3,4.$$

Proof. For $\mathcal{S}$ and $\mathcal{S}^\star$, we have from (9), gives

$$\begin{aligned} ||\mathcal{K}_1(\mathsf{s},\mathcal{S}) - \mathcal{K}_1(\mathsf{s},\mathcal{S}^\star)|| &= ||\alpha\mathcal{N} - \beta\mathcal{S}\mathcal{I} + \theta\mathcal{R} - \phi\mathcal{S} - (\alpha\mathcal{N} - \beta\mathcal{S}^\star\mathcal{I} + \theta\mathcal{R} - \phi\mathcal{S}^\star)|| \\ &\leq ||\beta\mathcal{I}(\mathsf{s})||||\mathcal{S}(\mathsf{s}) - \mathcal{S}^\star(\mathsf{s})|| + \phi||\mathcal{S}(\mathsf{s}) - \mathcal{S}^\star(\mathsf{s})|| \\ &\leq (\mathfrak{c}_3\beta + \phi)||\mathcal{S}(\mathsf{s}) - \mathcal{S}^\star(\mathsf{s})|| \\ &= \mathfrak{j}_1||\mathcal{S}(\mathsf{s}) - \mathcal{S}^\star(\mathsf{s})||, \end{aligned} \tag{11}$$

where $\mathfrak{j}_1 = \mathfrak{c}_3\beta + \phi$.
For $\mathcal{E}$ and $\mathcal{E}^\star$, we have

$$\begin{aligned} ||\mathcal{K}_2(\mathsf{s},\mathcal{E}) - \mathcal{K}_2(\mathsf{s},\mathcal{E}^\star)|| &= ||\beta\mathcal{S}\mathcal{I} - \gamma\mathcal{E} - \phi\mathcal{E} - (\beta\mathcal{S}\mathcal{I} - \gamma\mathcal{E}^\star - \phi\mathcal{E}^\star)|| \\ &\leq (\gamma + \phi)||\mathcal{E}(\mathsf{s}) - \mathcal{E}^\star(\mathsf{s})|| \\ &= \mathfrak{j}_2||\mathcal{E}(\mathsf{s}) - \mathcal{E}^\star(\mathsf{s})||, \end{aligned} \tag{12}$$

where $\mathfrak{j}_2 = \gamma + \phi$.
For $\mathcal{I}$ and $\mathcal{I}^\star$, we have

$$\begin{aligned} ||\mathcal{K}_3(\mathsf{s},\mathcal{I}) - \mathcal{K}_3(\mathsf{s},\mathcal{I}^\star)|| &= ||\gamma\mathcal{E} - \omega\mathcal{I} - \phi\mathcal{I} - (\gamma\mathcal{E} - \omega\mathcal{I}^\star - \phi\mathcal{I}^\star)|| \\ &\leq (\omega + \phi)||\mathcal{I}(\mathsf{s}) - \mathcal{I}^\star(\mathsf{s})|| \\ &= \mathfrak{j}_3||\mathcal{I}(\mathsf{s}) - \mathcal{I}^\star(\mathsf{s})||, \end{aligned} \tag{13}$$

where $\mathfrak{j}_3 = \omega + \phi$.
For $\mathcal{R}$ and $\mathcal{R}^\star$, we have

$$\begin{aligned} ||\mathcal{K}_4(\mathsf{s},\mathcal{R}) - \mathcal{K}_4(\mathsf{s},\mathcal{R}^\star)|| &= ||\omega\mathcal{I} - \theta\mathcal{R} - \phi\mathcal{R} - (\omega\mathcal{I} - \theta\mathcal{R}^\star - \phi\mathcal{R}^\star)|| \\ &\leq (\theta + \phi)||\mathcal{R}(\mathsf{s}) - \mathcal{R}^\star(\mathsf{s})|| \\ &= \mathfrak{j}_4||\mathcal{R}(\mathsf{s}) - \mathcal{R}^\star(\mathsf{s})||, \end{aligned} \tag{14}$$

where $\mathfrak{j}_4 = \theta + \phi$. Thus, from (11)-(14), we have that $\mathcal{K}_\mathfrak{i}$ for $\mathfrak{i} = 1,2,3,4$, satisfy the Lipschitz property.

Theorem 5. *There is at least a solution of the system* (1) *if* $\delta = \max\{\mathsf{j}_1, \mathsf{j}_2, \mathsf{j}_3, \mathsf{j}_4\} < 1$.

Proof. Let

$$\begin{aligned}
\lambda_{1\mathfrak{k}}(\mathsf{s}) &= \mathcal{S}_{\mathfrak{k}+1}(\mathsf{s}) - \mathcal{S}(\mathsf{s}),\\
\lambda_{2\mathfrak{k}}(\mathsf{s}) &= \mathcal{E}_{\mathfrak{k}+1}(\mathsf{s}) - \mathcal{E}(\mathsf{s}),\\
\lambda_{3\mathfrak{k}}(\mathsf{s}) &= \mathcal{I}_{\mathfrak{k}+1}(\mathsf{s}) - \mathcal{I}(\mathsf{s}),\\
\lambda_{4\mathfrak{k}}(\mathsf{s}) &= \mathcal{R}_{\mathfrak{k}+1}(\mathsf{s}) - \mathcal{R}(\mathsf{s}).
\end{aligned}$$

Then, we have

$$\begin{aligned}
||\lambda_{1\mathfrak{k}}(\mathsf{s})|| = ||\mathcal{S}_{\mathfrak{k}+1}(\mathsf{s}) - \mathcal{S}(\mathsf{s})|| &= \left\| \frac{2(1-\mathsf{a})}{(2-\mathsf{a})\mathcal{M}(\mathsf{a})}(\mathcal{K}_1(\mathsf{s}, \mathcal{S}_{\mathfrak{k}}) - \mathcal{K}_1(\mathsf{s}, \mathcal{S})) \right.\\
&\quad \left. + \frac{2\mathsf{a}}{(2-\mathsf{a})\mathcal{M}(\mathsf{a})} \int_0^{\mathsf{s}} (\mathcal{K}_1(\xi, \mathcal{S}_{\mathfrak{k}}) - \mathcal{K}_1(\xi, \mathcal{S}))d\xi \right\|\\
&\leq \frac{2(1-\mathsf{a})}{(2-\mathsf{a})\mathcal{M}(\mathsf{a})} \left\| \mathcal{K}_1(\mathsf{s}, \mathcal{S}_{\mathfrak{k}}) - \mathcal{K}_1(\mathsf{s}, \mathcal{S}) \right\|\\
&\quad + \frac{2\mathsf{a}}{(2-\mathsf{a})\mathcal{M}(\mathsf{a})} \int_0^{\mathsf{s}} \left\| \mathcal{K}_1(\xi, \mathcal{S}_{\mathfrak{k}}) - \mathcal{K}_1(\xi, \mathcal{S}) \right\| d\xi\\
&\leq \frac{2(1-\mathsf{a})}{(2-\mathsf{a})\mathcal{M}(\mathsf{a})} \mathsf{j}_1 ||\mathcal{S}_{\mathfrak{k}} - \mathcal{S}||\\
&\quad + \frac{2\mathsf{a}}{(2-\mathsf{a})\mathcal{M}(\mathsf{a})} \int_0^{\mathsf{s}} \mathsf{j}_1 ||\mathcal{S}_{\mathfrak{k}} - \mathcal{S}|| d\xi\\
&= \frac{2(1-\mathsf{a})}{(2-\mathsf{a})\mathcal{M}(\mathsf{a})} \mathsf{j}_1 ||\mathcal{S}_{\mathfrak{k}} - \mathcal{S}||\\
&\quad + \frac{2\mathsf{a}}{(2-\mathsf{a})\mathcal{M}(\mathsf{a})} \mathsf{j}_1 \int_0^{\mathsf{s}} ||\mathcal{S}_{\mathfrak{k}} - \mathcal{S}|| d\xi\\
&\leq \left(\frac{2(1-\mathsf{a})}{(2-\mathsf{a})\mathcal{M}(\mathsf{a})} + \frac{2\mathsf{a}\mathsf{s}}{(2-\mathsf{a})\mathcal{M}(\mathsf{a})} \right) \mathsf{j}_1 ||\mathcal{S}_{\mathfrak{k}} - \mathcal{S}||\\
&\leq \left(\frac{2(1-\mathsf{a})}{(2-\mathsf{a})\mathcal{M}(\mathsf{a})} + \frac{2\mathsf{a}\mathsf{s}}{(2-\mathsf{a})\mathcal{M}(\mathsf{a})} \right)^{\mathfrak{n}} \mathsf{j}_1^{\mathfrak{n}} ||\mathcal{S}_1 - \mathcal{S}||.
\end{aligned}$$

Since $\mathsf{j}_1 < 1$. As $\mathfrak{n} \to \infty$, we have $\mathcal{S}_{\mathfrak{n}} \to \mathcal{S}$. Similarly,

$$\begin{aligned}
||\lambda_{2\mathfrak{k}}(\mathsf{s})|| &\leq \left(\frac{2(1-\mathsf{a})}{(2-\mathsf{a})\mathcal{M}(\mathsf{a})} + \frac{2\mathsf{a}\mathsf{s}}{(2-\mathsf{a})\mathcal{M}(\mathsf{a})} \right)^{\mathfrak{n}} \mathsf{j}_2^{\mathfrak{n}} ||\mathcal{E}_1 - \mathcal{E}||\\
||\lambda_{3\mathfrak{k}}(\mathsf{s})|| &\leq \left(\frac{2(1-\mathsf{a})}{(2-\mathsf{a})\mathcal{M}(\mathsf{a})} + \frac{2\mathsf{a}\mathsf{s}}{(2-\mathsf{a})\mathcal{M}(\mathsf{a})} \right)^{\mathfrak{n}} \mathsf{j}_3^{\mathfrak{n}} ||\mathcal{I}_1 - \mathcal{I}||\\
||\lambda_{4\mathfrak{k}}(\mathsf{s})|| &\leq \left(\frac{2(1-\mathsf{a})}{(2-\mathsf{a})\mathcal{M}(\mathsf{a})} + \frac{2\mathsf{a}\mathsf{s}}{(2-\mathsf{a})\mathcal{M}(\mathsf{a})} \right)^{\mathfrak{n}} \mathsf{j}_4^{\mathfrak{n}} ||\mathcal{R}_1 - \mathcal{R}||.
\end{aligned}$$

As $\mathfrak{n} \to \infty$, we get $\lambda_{\mathfrak{i}\mathfrak{k}}(\mathsf{s}) \to 0$ with $\mathsf{j}_{\mathfrak{i}} < 1$ for $\mathfrak{i} = 1, 2, 3, 4$. Hence, the system (1) has a solution.

Theorem 6. *The system* (1) *has a unique solution if*

$$\left(\frac{2(1-\mathsf{a})}{(2-\mathsf{a})\mathcal{M}(\mathsf{a})}+\frac{2\mathsf{as}}{(2-\mathsf{a})\mathcal{M}(\mathsf{a})}\right)\mathrm{j}_{\mathfrak{i}}\leq 1,\ \textit{for}\ \mathfrak{i}=1,2,3,4.$$

Proof. Assume that there exists another solution $\mathcal{S}^{\star}(\mathsf{s}),\mathcal{E}^{\star}(\mathsf{s}),\mathcal{I}^{\star}(\mathsf{s}),\mathcal{R}^{\star}(\mathsf{s})$ *with initial values such that*

$$\begin{aligned}
\mathcal{S}^{\star}(\mathsf{s})&=\mathcal{S}(0)+\frac{2(1-\mathsf{a})}{(2-\mathsf{a})\mathcal{M}(\mathsf{a})}\mathcal{K}_1(\mathsf{s},\mathcal{S}^{\star})+\frac{2\mathsf{a}}{(2-\mathsf{a})\mathcal{M}(\mathsf{a})}\int_0^{\mathsf{s}}\mathcal{K}_1(\xi,\mathcal{S}^{\star})d\xi,\\
\mathcal{E}^{\star}(\mathsf{s})&=\mathcal{E}(0)+\frac{2(1-\mathsf{a})}{(2-\mathsf{a})\mathcal{M}(\mathsf{a})}\mathcal{K}_2(\mathsf{s},\mathcal{E}^{\star})+\frac{2\mathsf{a}}{(2-\mathsf{a})\mathcal{M}(\mathsf{a})}\int_0^{\mathsf{s}}\mathcal{K}_2(\xi,\mathcal{E}^{\star})d\xi,\\
\mathcal{I}^{\star}(\mathsf{s})&=\mathcal{I}(0)+\frac{2(1-\mathsf{a})}{(2-\mathsf{a})\mathcal{M}(\mathsf{a})}\mathcal{K}_3(\mathsf{s},\mathcal{I}^{\star})+\frac{2\mathsf{a}}{(2-\mathsf{a})\mathcal{M}(\mathsf{a})}\int_0^{\mathsf{s}}\mathcal{K}_3(\xi,\mathcal{I}^{\star})d\xi\\
\mathcal{R}^{\star}(\mathsf{s})&=\mathcal{R}(0)+\frac{2(1-\mathsf{a})}{(2-\mathsf{a})\mathcal{M}(\mathsf{a})}\mathcal{K}_4(\mathsf{s},\mathcal{R}^{\star})+\frac{2\mathsf{a}}{(2-\mathsf{a})\mathcal{M}(\mathsf{a})}\int_0^{\mathsf{s}}\mathcal{K}_4(\xi,\mathcal{R}^{\star})d\xi.
\end{aligned}$$

Now,

$$\begin{aligned}
||\mathcal{S}-\mathcal{S}^{\star}||&=\left\|\frac{2(1-\mathsf{a})}{(2-\mathsf{a})\mathcal{M}(\mathsf{a})}(\mathcal{K}_1(\mathsf{s},\mathcal{S})-\mathcal{K}_1(\mathsf{s},\mathcal{S}^{\star}))\right.\\
&\quad\left.+\frac{2\mathsf{a}}{(2-\mathsf{a})\mathcal{M}(\mathsf{a})}\int_0^{\mathsf{s}}(\mathcal{K}_1(\xi,\mathcal{S})-\mathcal{K}_1(\xi,\mathcal{S}^{\star}))d\xi\right\|\\
&\leq\frac{2(1-\mathsf{a})}{(2-\mathsf{a})\mathcal{M}(\mathsf{a})}\left\|\mathcal{K}_1(\mathsf{s},\mathcal{S})-\mathcal{K}_1(\mathsf{s},\mathcal{S}^{\star})\right\|\\
&\quad+\frac{2\mathsf{a}}{(2-\mathsf{a})\mathcal{M}(\mathsf{a})}\int_0^{\mathsf{s}}\left\|\mathcal{K}_1(\xi,\mathcal{S})-\mathcal{K}_1(\xi,\mathcal{S}^{\star}))\right\|d\xi\\
&\leq\frac{2(1-\mathsf{a})}{(2-\mathsf{a})\mathcal{M}(\mathsf{a})}\mathrm{j}_1||\mathcal{S}-\mathcal{S}^{\star}||\\
&\quad+\frac{2\mathsf{a}}{(2-\mathsf{a})\mathcal{M}(\mathsf{a})}\int_0^{\mathsf{s}}\mathrm{j}_1||\mathcal{S}-\mathcal{S}^{\star}||d\xi\\
&=\frac{2(1-\mathsf{a})}{(2-\mathsf{a})\mathcal{M}(\mathsf{a})}\mathrm{j}_1||\mathcal{S}-\mathcal{S}^{\star}||\\
&\quad+\frac{2\mathsf{a}}{(2-\mathsf{a})\mathcal{M}(\mathsf{a})}\mathrm{j}_1\int_0^{\mathsf{s}}||\mathcal{S}-\mathcal{S}^{\star}||d\xi\\
&\leq\left(\frac{2(1-\mathsf{a})}{(2-\mathsf{a})\mathcal{M}(\mathsf{a})}+\frac{2\mathsf{as}}{(2-\mathsf{a})\mathcal{M}(\mathsf{a})}\right)\mathrm{j}_1||\mathcal{S}-\mathcal{S}^{\star}||\\
&\leq\left(\frac{2(1-\mathsf{a})}{(2-\mathsf{a})\mathcal{M}(\mathsf{a})}+\frac{2\mathsf{as}}{(2-\mathsf{a})\mathcal{M}(\mathsf{a})}\right)\mathrm{j}_1||\mathcal{S}-\mathcal{S}^{\star}||,
\end{aligned}$$

which implies that

$$\left(1-\left(\frac{2(1-\mathsf{a})}{(2-\mathsf{a})\mathcal{M}(\mathsf{a})}+\frac{2\mathsf{as}}{(2-\mathsf{a})\mathcal{M}(\mathsf{a})}\right)\mathrm{j}_1\right)||\mathcal{S}-\mathcal{S}^{\star}||\leq 0.$$

Therefore, $||\mathcal{S}-\mathcal{S}^{\star}||=0$. *Hence,* $\mathcal{S}=\mathcal{S}^{\star}$. *Similarly, we can prove*

$$\mathcal{V}=\mathcal{V}^{\star},\mathcal{E}=\mathcal{E}^{\star},\mathcal{I}=\mathcal{I}^{\star},\mathcal{R}=\mathcal{R}^{\star}.$$

Hence, the system (1) *has a unique solution.*

3. Ulam-Hyers stability

In this section, we obtain the Ulam-Hyers stability of the system (1). We state the required definition.

Definition 6. *The system* (1) *has Ulam-Hyers stability if there exist constants* $\mathcal{K}_{\mathfrak{i}}>0$, $\mathfrak{i}=1,2,3,4$ *satisfying: For every* $\epsilon_{\mathfrak{i}}>0$, $\mathfrak{i}=1,2,3,4$, *if*

$$\begin{cases} \left|{}^{\mathfrak{CF}}_{\quad}\mathcal{D}^{\mathsf{a}}_{\mathsf{s}}\mathcal{S}(\mathsf{s})-\mathcal{K}_1(\mathsf{s},\mathcal{S})\right|\leq\epsilon_1,\\ \left|{}^{\mathfrak{CF}}_{\quad}\mathcal{D}^{\mathsf{a}}_{\mathsf{s}}\mathcal{E}(\mathsf{s})-\mathcal{K}_2(\mathsf{s},\mathcal{E})\right|\leq\epsilon_2,\\ \left|{}^{\mathfrak{CF}}_{\quad}\mathcal{D}^{\mathsf{a}}_{\mathsf{s}}\mathcal{I}(\mathsf{s})-\mathcal{K}_3(\mathsf{s},\mathcal{I})\right|\leq\epsilon_3,\\ \left|{}^{\mathfrak{CF}}_{\quad}\mathcal{D}^{\mathsf{a}}_{\mathsf{s}}\mathcal{R}(\mathsf{s})-\mathcal{K}_4(\mathsf{s},\mathcal{R})\right|\leq\epsilon_4, \end{cases} \tag{15}$$

and there exists a solution of the system (1), $\mathcal{S}^{\star}(\mathsf{s}),\mathcal{E}^{\star}(\mathsf{s}),\mathcal{I}^{\star}(\mathsf{s})$ *and* $\mathcal{R}^{\star}(\mathsf{s})$ *that statisfying the given model, such that*

$$||\mathcal{S}-\mathcal{S}^{\star}||\leq\eta_1\epsilon_1,||\mathcal{E}-\mathcal{E}^{\star}||\leq\eta_2\epsilon_2,$$
$$||\mathcal{I}-\mathcal{I}^{\star}||\leq\eta_3\epsilon_3,||\mathcal{R}-\mathcal{R}^{\star}||\leq\eta_4\epsilon_4.$$

Remark 1. *Consider that function* $\mathcal{S}$ *is a solution of the first inequality* (15) *iff a continuous function* $\mathfrak{h}_1$ *exists (depending on* $\mathcal{S}_1$*) so that*

(i) $|\mathfrak{h}_1(\mathsf{s})|<\epsilon_1$, *and*

(ii) ${}^{\mathfrak{CF}}\mathcal{D}^{\mathsf{a}}_{\mathsf{s}}\mathcal{S}(\mathsf{s})=\mathcal{W}_1(\mathsf{s},\mathcal{S})+\mathfrak{h}_1(\mathsf{s})$.

Similarly, we can define for other classes of the model (15) *for some* $\mathfrak{h}_{\mathfrak{i}}$ *where* $\mathfrak{i}=2,3,4$.

Theorem 7. *Assume that the hypothesis* $(\mathcal{G})$ *holds true. Then the system* (1) *is Ulam-Hyers stable if*

$$\left(\frac{2(1-\mathsf{a})}{(2-\mathsf{a})\mathcal{M}(\mathsf{a})}+\frac{2\mathsf{as}}{(2-\mathsf{a})\mathcal{M}(\mathsf{a})}\right)\mathfrak{j}_{\mathfrak{i}}\leq 1,\ \textit{for}\ \mathfrak{i}=1,2,3,4.$$

Proof. Let $\epsilon_1>0$ *and the function* $\mathcal{S}$ *be arbitary such that*

$$\left|{}^{\mathfrak{CF}}_{\quad}\mathcal{D}^{\mathsf{a}}_{\mathsf{s}}\mathcal{S}(\mathsf{s})-\mathcal{K}_1(\mathsf{s},\mathcal{S})\right|\leq\epsilon_1.$$

According to Remark 1, we have a function $\mathfrak{h}_1$ *with* $|\mathfrak{h}_1| < \epsilon_1$*, which satisfies*

$$^{\mathfrak{CF}}\mathcal{D}^{\mathsf{a}}_{\mathsf{s}}\mathcal{S}(\mathsf{s}) = \mathcal{W}_1(\mathsf{s}, \mathcal{S}) + \mathfrak{h}_1(\mathsf{s}).$$

Accordingly, we get

$$\begin{aligned}\mathcal{S}(\mathsf{s}) = \mathcal{S}(0) &+ \frac{2(1-\mathsf{a})}{(2-\mathsf{a})\mathcal{M}(\mathsf{a})}\mathcal{K}_1(\mathsf{s}, \mathcal{S}(\mathsf{s})) + \frac{2\mathsf{a}}{(2-\mathsf{a})\mathcal{M}(\mathsf{a})}\int_0^{\mathsf{s}} \mathcal{K}_1(\xi, \mathcal{S}(\mathsf{s}))d\xi \\ &+ \frac{2(1-\mathsf{a})}{(2-\mathsf{a})\mathcal{M}(\mathsf{a})}\mathfrak{h}_1(\mathsf{s}) + \frac{2\mathsf{a}}{(2-\mathsf{a})\mathcal{M}(\mathsf{a})}\int_0^{\mathsf{s}} \mathfrak{h}_1(\xi)d\xi.\end{aligned}$$

Let $\mathcal{S}^\star$ *be the unique solution of the system* (1)*. Then,*

$$\mathcal{S}^\star(\mathsf{s}) = \mathcal{S}(0) + \frac{2(1-\mathsf{a})}{(2-\mathsf{a})\mathcal{M}(\mathsf{a})}\mathcal{K}_1(\mathsf{s}, \mathcal{S}^\star(\mathsf{s})) + \frac{2\mathsf{a}}{(2-\mathsf{a})\mathcal{M}(\mathsf{a})}\int_0^{\mathsf{s}} \mathcal{K}_1(\xi, \mathcal{S}^\star(\mathsf{s}))d\xi.$$

Hence,

$$\begin{aligned}|\mathcal{S}(\mathsf{s}) - \mathcal{S}^\star(\mathsf{s})| &\leq \frac{2(1-\mathsf{a})}{(2-\mathsf{a})\mathcal{M}(\mathsf{a})}|\mathcal{K}_1(\mathsf{s}, \mathcal{S}(\mathsf{s})) - \mathcal{K}_1(\mathsf{s}, \mathcal{S}^\star(\mathsf{s}))| \\ &+ \frac{2\mathsf{a}}{(2-\mathsf{a})\mathcal{M}(\mathsf{a})}\int_0^{\mathsf{s}} |\mathcal{K}_1(\xi, \mathcal{S}(\mathsf{s})) - \mathcal{K}_1(\xi, \mathcal{S}^\star(\mathsf{s}))|d\xi \\ &+ \frac{2(1-\mathsf{a})}{(2-\mathsf{a})\mathcal{M}(\mathsf{a})}|\mathfrak{h}_1(\mathsf{s})| + \frac{2\mathsf{a}}{(2-\mathsf{a})\mathcal{M}(\mathsf{a})}\int_0^{\mathsf{s}} |\mathfrak{h}_1(\xi)|d\xi \\ &\leq \left[\frac{2(1-\mathsf{a})}{(2-\mathsf{a})\mathcal{M}(\mathsf{a})} + \frac{2\mathsf{a}\mathsf{s}}{(2-\mathsf{a})\mathcal{M}(\mathsf{a})}\right]\mathfrak{j}_1|\mathcal{S}(\mathsf{s}) - \mathcal{S}^\star(\mathsf{s})| \\ &+ \left[\frac{2(1-\mathsf{a})}{(2-\mathsf{a})\mathcal{M}(\mathsf{a})} + \frac{2\mathsf{a}\mathsf{s}}{(2-\mathsf{a})\mathcal{M}(\mathsf{a})}\right]\epsilon_1 \\ ||\mathcal{S}(\mathsf{s}) - \mathcal{S}^\star(\mathsf{s})|| &\leq \frac{\left[\frac{2(1-\mathsf{a})}{(2-\mathsf{a})\mathcal{M}(\mathsf{a})} + \frac{2\mathsf{a}\mathsf{s}}{(2-\mathsf{a})\mathcal{M}(\mathsf{a})}\right]\epsilon_1}{1 - \left[\frac{2(1-\mathsf{a})}{(2-\mathsf{a})\mathcal{M}(\mathsf{a})} + \frac{2\mathsf{a}\mathsf{s}}{(2-\mathsf{a})\mathcal{M}(\mathsf{a})}\right]\mathfrak{j}_1}.\end{aligned}$$

Then,

$$||\mathcal{S}(\mathsf{s}) - \mathcal{S}^\star(\mathsf{s})|| \leq \eta_1\epsilon_1,$$

where

$$\eta_1 = \frac{\left[\frac{2(1-\mathsf{a})}{(2-\mathsf{a})\mathcal{M}(\mathsf{a})} + \frac{2\mathsf{a}\mathsf{s}}{(2-\mathsf{a})\mathcal{M}(\mathsf{a})}\right]}{1 - \left[\frac{2(1-\mathsf{a})}{(2-\mathsf{a})\mathcal{M}(\mathsf{a})} + \frac{2\mathsf{a}\mathsf{s}}{(2-\mathsf{a})\mathcal{M}(\mathsf{a})}\right]\mathfrak{j}_1}.$$

Similarly, we have

$$||\mathcal{E} - \mathcal{E}^\star|| \leq \eta_2\epsilon_2, ||\mathcal{I} - \mathcal{I}^\star|| \leq \eta_3\epsilon_3, ||\mathcal{R} - \mathcal{R}^\star|| \leq \eta_4\epsilon_4.$$

Thus, the system (1) *is Ulam-Hyers stable.*

4. Equilibrium points

This section investigate the disease-free and disease-endemic equilibrium points of the system (1) to identify the infected state of the disease. Disease-Free Equilibrium(DFE) points of the system are calculated by using the assumptions: ${}^{\mathfrak{CF}}\mathcal{D}_{\mathsf{s}}^{\mathsf{a}}\mathcal{S} = 0, {}^{\mathfrak{CF}}\mathcal{D}_{\mathsf{s}}^{\mathsf{a}}\mathcal{E} = 0, {}^{\mathfrak{CF}}\mathcal{D}_{\mathsf{s}}^{\mathsf{a}}\mathcal{I} = 0, {}^{\mathfrak{CF}}\mathcal{D}_{\mathsf{s}}^{\mathsf{a}}\mathcal{R} = 0$

$$\begin{cases} \alpha\mathcal{N} - \beta\mathcal{S}\mathcal{I} + \theta\mathcal{R} - \phi\mathcal{S} = 0 \\ \beta\mathcal{S}\mathcal{I} - \gamma\mathcal{E} - \phi\mathcal{E} = 0 \\ \gamma\mathcal{E} - \omega\mathcal{I} - \phi\mathcal{I} = 0, \\ \omega\mathcal{I} - \theta\mathcal{R} - \phi\mathcal{R} = 0 \end{cases}$$

Let $\mathcal{E} = \mathcal{I} = 0$, to find the Disease Free Equilibrium, $(\mathcal{S}_0, \mathcal{E}_0, \mathcal{I}_0, \mathcal{R}_0) = \left(\frac{\alpha\mathcal{N}}{\phi}, 0, 0, 0\right)$ Now, the Disease-Endemic equilibrium (DEE) is:

$$(\mathcal{S}^*, \mathcal{E}^*, \mathcal{I}^*, \mathcal{R}^*) = \left(\frac{(\gamma+\phi)(\omega+\phi)}{\beta\gamma}, \left(\frac{\omega+\phi}{\gamma}\right)\mathcal{I}, \mathcal{I}, \left(\frac{\omega}{\theta+\phi}\right)\right)$$

The disease-free equilibrium is locally asymptotically stable if either $\mathcal{R}_0 < 1$; if not, it will be unstable, according to the stability analyses. However, when $\mathcal{R}_0 > 1$, the disease-endemic equilibrium point is locally asymptotically stable; if not, it can be unstable.

4.1. Stability of Equilibria

Theorem 8. *The DFE is locally asymptotically stable if $\mathcal{R}_0 < 1$ and unstable if $\mathcal{R}_0 > 1$.*

Proof. The Jacobian at DFE:

$$\mathcal{J} = \begin{pmatrix} -\phi & 0 & -\beta\mathcal{S}_0 & \theta \\ 0 & -(\gamma+\phi) & \beta\mathcal{S}_0 & 0 \\ 0 & \gamma & -(\omega+\phi) & 0 \\ 0 & 0 & \omega & -(\theta+\phi) \end{pmatrix}$$

The characteristic equation gives eigenvalues:

$$\lambda^2 + (\gamma+\omega+2\phi)\lambda + (\gamma+\phi)(\omega+\phi)(1-\mathcal{R}_0) = 0$$

For $\mathcal{R}_0 < 1$, all eigenvalues have negative real parts.

Theorem 9. *When $\mathcal{R}_0 > 1$, the endemic equilibrium $\mathcal{E}^*$ is locally asymptotically stable.*

Proof. The Jacobian at EE satisfies:

$$\mathrm{tr}(\mathcal{J}^*) = -(\phi + \beta\mathcal{I}^* + \gamma + \phi + \omega + \phi + \theta + \phi) < 0$$

and $\det(\mathcal{J}^*) > 0$ when $\mathcal{R}_0 > 1$, proving stability.

4.2. Basic reproduction number $\mathcal{R}_0$

$\mathcal{R}_0$ is essential parameter in epidemiology to illustrate the behavior of disease. It is found by evaluating the dominant eigenvalue of the next generation matrix from the DFE. In this calculation part, consider

$$\begin{cases} {}^{\mathfrak{C}\mathfrak{F}}\mathcal{D}_{\mathsf{s}}^{\mathsf{a}}\mathcal{E} & = \beta\mathcal{S}\mathcal{I} - \gamma\mathcal{E} - \phi\mathcal{E}, \\ {}^{\mathfrak{C}\mathfrak{F}}\mathcal{D}_{\mathsf{s}}^{\mathsf{a}}\mathcal{I} & = \gamma\mathcal{E} - \omega\mathcal{I} - \phi\mathcal{I}, \end{cases} \tag{16}$$

Now,

$$\mathsf{F} = \begin{bmatrix} \beta\mathcal{S}\mathcal{I} \\ 0 \end{bmatrix} \text{ and } \mathsf{V} = \begin{bmatrix} (\gamma+\phi)\mathcal{E} \\ -\gamma\mathcal{E} + (\omega+\phi)\mathcal{I} \end{bmatrix}$$

Then,

$$\mathbb{F} = \begin{bmatrix} 0 & \beta \\ 0 & 0 \end{bmatrix} \text{ and } \mathbb{V}^{-1} = \frac{1}{(\gamma+\phi)((\omega+\phi)} \begin{bmatrix} (\omega+\phi) & 0 \\ -\gamma & (\gamma+\phi) \end{bmatrix}$$

$$\therefore \mathbb{F}\mathbb{V}^{-1} = \begin{bmatrix} \dfrac{\beta\gamma}{(\gamma+\phi)(\omega+\phi)} & \dfrac{\beta}{(\omega+\phi)} \\ 0 & 0 \end{bmatrix}$$

Hence, $\mathcal{R}_0 = \rho(\mathbb{F}\mathbb{V}^{-1}) = \dfrac{\beta\gamma}{(\gamma+\phi)(\omega+\phi)}$.

4.3. Sensitivity analysis of the reproduction number $\mathcal{R}_0$

To investigate the influence of key transmission dynamics of the system, sensitivity analysis of the basic reproduction number $\mathcal{R}_0$ with respect to each parameter was computed by:

$$\Upsilon_{\mathsf{p}}^{\mathcal{R}_0} = \frac{\partial\mathcal{R}_0}{\partial\mathsf{p}} \cdot \frac{\mathsf{p}}{\mathcal{R}_0},$$

where p represents each parameter. This sensitivity index quantifies the relative change in $\mathcal{R}_0$ due to a relative change in the parameter p. In Figure 2, a positive sensitivity index indicates that increasing the parameter leads to increase in $\mathcal{R}_0$, while a negative index indicates the opposite. Parameters with sensitivity indices closer to +1 or -1 have a stronger influence on $\mathcal{R}_0$. In particular, Figure 3 illustrates the 3D surface of $\mathcal{R}_0$ over a range of parameter values $\beta \in [0.001, 0.1]$ and $\gamma \in [0.01, 0.3]$. The red curve denotes the epidemic threshold $\mathcal{R}_0 = 1$. Regions above this threshold suggest potential for disease spread, whereas regions below imply containment. Figure 3 highlights how $\mathcal{R}_0$ increases monotonically as β grows and decreases as γ increases.

When $\mathcal{R}_0 > 1$, the disease can spread in the population, whereas $\mathcal{R}_0 < 1$, indicates eventual disease elimination.

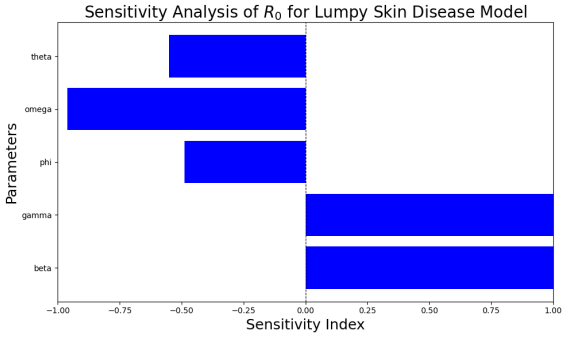

Figure 2: Sensitivity Analysis of R_0 with key parameters

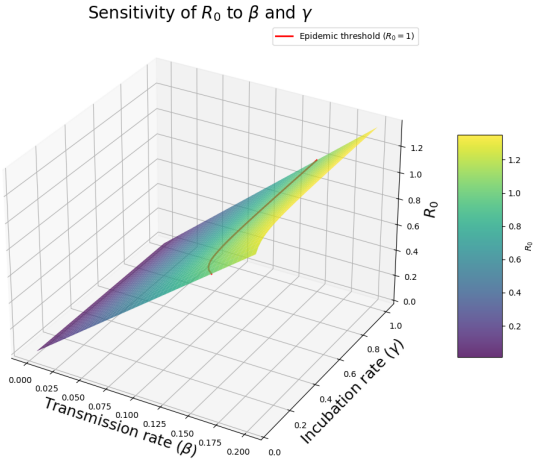

Figure 3: Sensitivity Analysis of $\mathcal{R}_0$ to Transmission rate (β) and Incubation rate (γ)

5. Numerical scheme

Here, a numerical scheme for the system (1) is developed. For this, we use the approach related to Newton interpolation polynomials. Consider a general Cauchy problem with fractal fractional differential operator as:

$$\begin{cases} {}^{\mathfrak{CF}}\mathcal{D}^{\mathsf{a}}_{\mathsf{s}}\phi(\mathsf{s}) = \mathcal{K}(\mathsf{s}, \phi(\mathsf{s})) \\ \phi(0) = \phi_0. \end{cases} \tag{17}$$

Utilizing the fractal fractional integral operator, we obtain

$$\phi(\mathsf{s}) = \phi(0) + \frac{2(1-\mathsf{a})}{(2-\mathsf{a})\mathcal{M}(\mathsf{a})}\mathcal{K}(\mathsf{s}, \phi(\mathsf{s})) + \frac{2\mathsf{a}}{(2-\mathsf{a})\mathcal{M}(\mathsf{a})}\int_0^{\mathsf{s}} \mathcal{K}(\xi, \phi(\xi))d\xi.$$

Putting s by $\mathsf{s}_{\mathfrak{n}+1}$, which gives

$$\phi_{\mathfrak{n}+1} = \phi(0) + \frac{2(1-\mathsf{a})}{(2-\mathsf{a})\mathcal{M}(\mathsf{a})}\mathcal{K}(\mathsf{s}_{\mathfrak{n}}, \phi(\mathsf{s}_{\mathfrak{n}})) + \frac{2\mathsf{a}}{(2-\mathsf{a})\mathcal{M}(\mathsf{a})}\int_0^{\mathsf{s}_{\mathfrak{n}+1}} \mathcal{K}(\mathsf{s}, \phi(\mathsf{s}))d\mathsf{s}.$$

The successive terms difference is given as follows:

$$\phi_{\mathfrak{n}+1} - \phi_{\mathfrak{n}} = \frac{2(1-\mathsf{a})}{(2-\mathsf{a})\mathcal{M}(\mathsf{a})}(\mathcal{K}(\mathsf{s}_{\mathfrak{n}}, \phi_{\mathfrak{n}}) - \mathcal{K}(\mathsf{s}_{\mathfrak{n}-1}, \phi_{\mathfrak{n}-1})) + \frac{2\mathsf{a}}{(2-\mathsf{a})\mathcal{M}(\mathsf{a})} \int_{\mathsf{s}_{\mathfrak{n}}}^{\mathsf{s}_{\mathfrak{n}+1}} \mathcal{K}(\mathsf{s}, \phi(\mathsf{s}))d\mathsf{s}. \tag{18}$$

Over the closed interval $[\mathsf{s}_{\mathfrak{m}}, \mathsf{s}_{\mathfrak{m}+1}]$, the function $\mathcal{K}(\xi, \phi(\xi))$ can be approximated by the interpolation polynomial

$$\theta_{\mathfrak{m}}(\mathsf{s}) \cong \frac{\mathfrak{g}(\mathsf{s}_{\mathfrak{m}}, \mathfrak{y}_{\mathfrak{m}})}{\mathfrak{h}}(\mathsf{s} - \mathsf{s}_{\mathfrak{m}-1}) - \frac{\mathfrak{g}(\mathsf{s}_{\mathfrak{m}-1}, \mathfrak{y}_{\mathfrak{m}-1})}{\mathfrak{h}}(\mathsf{s} - \mathsf{s}_{\mathfrak{m}}), \tag{19}$$

where $\mathfrak{h} = \mathsf{s}_{\mathfrak{m}} - \mathsf{s}_{\mathfrak{m}-1}$. Consequently,

$$\begin{aligned}\int_{\mathsf{s}_{\mathfrak{n}}}^{\mathsf{s}_{\mathfrak{n}+1}} \mathcal{K}(\mathsf{s}, \phi(\mathsf{s}))d\mathsf{s} &= \int_{\mathsf{s}_{\mathfrak{n}}}^{\mathsf{s}_{\mathfrak{n}+1}} \left(\frac{\mathcal{K}(\mathsf{s}_{\mathfrak{n}}, \phi_{\mathfrak{n}})}{\mathfrak{h}}(\mathsf{s} - \mathsf{s}_{\mathfrak{n}-1}) - \right. \\ &\quad \left. \frac{\mathcal{K}(\mathsf{s}_{\mathfrak{n}-1}, \phi_{\mathfrak{n}-1})}{\mathfrak{h}}(\mathsf{s} - \mathsf{s}_{\mathfrak{n}}) \right) d\mathsf{s} \\ &= \frac{3\mathfrak{h}}{2}\mathcal{K}(\mathsf{s}_{\mathfrak{n}}, \phi_{\mathfrak{n}}) - \frac{\mathfrak{h}}{2}\mathcal{K}(\mathsf{s}_{\mathfrak{n}-1}, \phi_{\mathfrak{n}-1}).\end{aligned} \tag{20}$$

Putting (20) in (18) and after simplification, we get

$$\begin{aligned}\phi_{\mathfrak{n}+1} = \phi_{\mathfrak{n}} &+ \left(\frac{2(1-\mathsf{a})}{(2-\mathsf{a})\mathcal{M}(\mathsf{a})} + \frac{3\mathsf{a}\mathfrak{h}}{(2-\mathsf{a})\mathcal{M}(\mathsf{a})} \right) \mathcal{K}(\mathsf{s}_{\mathfrak{n}}, \phi_{\mathfrak{n}}) \\ &- \left(\frac{2(1-\mathsf{a})}{(2-\mathsf{a})\mathcal{M}(\mathsf{a})} + \frac{\mathsf{a}\mathfrak{h}}{(2-\mathsf{a})\mathcal{M}(\mathsf{a})} \right) \mathcal{K}(\mathsf{s}_{\mathfrak{n}-1}, \phi_{\mathfrak{n}-1}).\end{aligned}$$

Component-wise Representation Using Kernels

We now express the right-hand side of the system (10) in terms of kernel functions for each epidemiological class.

$$\begin{cases} \mathcal{K}_1(\mathsf{s}, \mathcal{S}) &= \alpha\mathcal{N} - \beta\mathcal{S}\mathcal{I} + \theta\mathcal{R} - \phi\mathcal{S}, \\ \mathcal{K}_2(\mathsf{s}, \mathcal{E}) &= \beta\mathcal{S}\mathcal{I} - \gamma\mathcal{E} - \phi\mathcal{E}, \\ \mathcal{K}_3(\mathsf{s}, \mathcal{I}) &= \gamma\mathcal{E} - \omega\mathcal{I} - \phi\mathcal{I}, \\ \mathcal{K}_4(\mathsf{s}, \mathcal{R}) &= \omega\mathcal{I} - \theta\mathcal{R} - \phi\mathcal{R}. \end{cases}$$

where Λ, β, δ, γ, and μ are the respective model parameters. These kernels represent the instantaneous rate of change in each compartment and are used in the numerical scheme via their evaluations at discrete time steps. Hence, the numerical scheme for (10) is obtained as the following:

$$\mathcal{S}_{\mathfrak{n}+1} = \mathcal{S}_{\mathfrak{n}} + \left(\frac{2(1-\mathsf{a})}{(2-\mathsf{a})\mathcal{M}(\mathsf{a})} + \frac{3\mathsf{a}\mathfrak{h}}{(2-\mathsf{a})\mathcal{M}(\mathsf{a})} \right) \mathcal{K}_1(\mathsf{s}_{\mathfrak{n}}, \mathcal{S}_{\mathfrak{n}})$$

$$- \left(\frac{2(1-\mathsf{a})}{(2-\mathsf{a})\mathcal{M}(\mathsf{a})} + \frac{\mathsf{a}\mathfrak{h}}{(2-\mathsf{a})\mathcal{M}(\mathsf{a})} \right) \mathcal{K}_1(\mathsf{s}_{\mathfrak{n}-1}, \mathcal{S}_{\mathfrak{n}-1}),$$

$$\mathcal{E}_{\mathfrak{n}+1} = \mathcal{E}_{\mathfrak{n}} + \left(\frac{2(1-\mathsf{a})}{(2-\mathsf{a})\mathcal{M}(\mathsf{a})} + \frac{3\mathsf{a}\mathfrak{h}}{(2-\mathsf{a})\mathcal{M}(\mathsf{a})} \right) \mathcal{K}_2(\mathsf{s}_{\mathfrak{n}}, \mathcal{E}_{\mathfrak{n}})$$
$$- \left(\frac{2(1-\mathsf{a})}{(2-\mathsf{a})\mathcal{M}(\mathsf{a})} + \frac{\mathsf{a}\mathfrak{h}}{(2-\mathsf{a})\mathcal{M}(\mathsf{a})} \right) \mathcal{K}_2(\mathsf{s}_{\mathfrak{n}-1}, \mathcal{E}_{\mathfrak{n}-1}),$$

‘

$$\mathcal{I}_{\mathfrak{n}+1} = \mathcal{I}_{\mathfrak{n}} + \left(\frac{2(1-\mathsf{a})}{(2-\mathsf{a})\mathcal{M}(\mathsf{a})} + \frac{3\mathsf{a}\mathfrak{h}}{(2-\mathsf{a})\mathcal{M}(\mathsf{a})} \right) \mathcal{K}_3(\mathsf{s}_{\mathfrak{n}}, \mathcal{I}_{\mathfrak{n}})$$
$$- \left(\frac{2(1-\mathsf{a})}{(2-\mathsf{a})\mathcal{M}(\mathsf{a})} + \frac{\mathsf{a}\mathfrak{h}}{(2-\mathsf{a})\mathcal{M}(\mathsf{a})} \right) \mathcal{K}_3(\mathsf{s}_{\mathfrak{n}-1}, \mathcal{I}_{\mathfrak{n}-1}),$$

‘

$$\mathcal{R}_{\mathfrak{n}+1} = \mathcal{R}_{\mathfrak{n}} + \left(\frac{2(1-\mathsf{a})}{(2-\mathsf{a})\mathcal{M}(\mathsf{a})} + \frac{3\mathsf{a}\mathfrak{h}}{(2-\mathsf{a})\mathcal{M}(\mathsf{a})} \right) \mathcal{K}_4(\mathsf{s}_{\mathfrak{n}}, \mathcal{R}_{\mathfrak{n}})$$
$$- \left(\frac{2(1-\mathsf{a})}{(2-\mathsf{a})\mathcal{M}(\mathsf{a})} + \frac{\mathsf{a}\mathfrak{h}}{(2-\mathsf{a})\mathcal{M}(\mathsf{a})} \right) \mathcal{K}_4(\mathsf{s}_{\mathfrak{n}-1}, \mathcal{R}_{\mathfrak{n}-1}).$$

6. Results and discussion

We analyzed the system (1) to understand disease propagation dynamics in the current study. This model was explored to investigate the dynamics of disease within a population, and several results were validated through our analysis. The detailed mathematical model enables observation of model changes when fractional parameters transform. The numerical model results are provided in this section, using the parameter values listed in Table 1 and specified bounds for a. Also, a. Assumed initial values are:

$$\mathcal{S}(0) = 43815, \mathcal{E}(0) = 1, \mathcal{I}(0) = 1, \mathcal{R}(0) = 0,$$

Figure 4 demonstrates the dynamics of $\mathcal{S}, \mathcal{E}, \mathcal{I}$, and $\mathcal{R}$ at the fractional order at $\mathfrak{a} = 0.8$. In the susceptible population rapidly declines as individuals become exposed. The sharp drop in $\mathcal{S}(\mathsf{s})$ reflects a high transmission rate at early stages. A small portion stabilizes around a constant value, indicating a residual susceptible group that avoids infection due to herd effects or immunity. In the $\mathcal{E}(\mathsf{s})$, a peak is observed around $\mathsf{s} = 5$, after $\mathcal{E}(\mathsf{s})$ declines as individuals move into the infectious stage. In the $\mathcal{I}(\mathsf{s})$, peaks slightly later than the exposed group, around $\mathsf{s} = 10$, followed by a decay to a steady level. This shows that while infections spreads rapidly, recovery eventually stabilizes the epidemic. Recovery $\mathcal{R}(\mathsf{s})$ begins quickly, and the curves saturates near $\mathsf{s} = 50$, indicating most individuals have recovered. This reflects effective immune response or intervention strategies.

Figure 5 shows the comparison of the Newton interpolation scheme and the Finite Difference Method for simulating the infected population $\mathcal{I}(\mathsf{s})$ at $\mathfrak{a} = 0.8$. The Newton

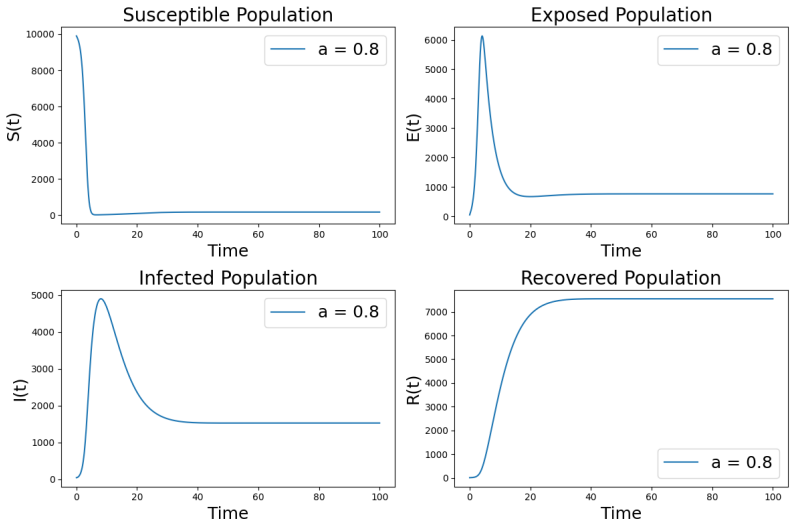

Figure 4: SEIR classes

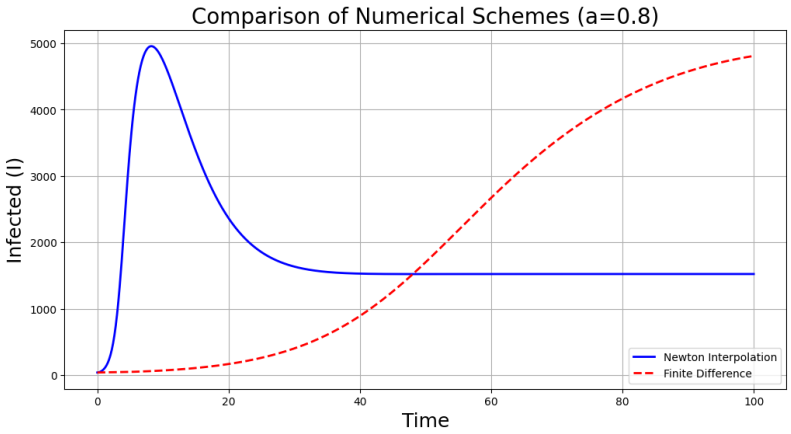

Figure 5: Comparison of results obtained by Newton interpolation and FDM scheme

method captures the infection peak earlier and reflects a realistic decay toward equilibrium, while the Finite Difference Method shows a delayed and continuously increasing infection trend. This suggests that Newton interpolation more accurately represents the transient dynamics of disease spread. Additionally, it offers better stability and responsiveness, making it more suitable for fractional-order models where memory effects are significant.

Moreover, a convergence analysis was performed for the proposed numerical scheme applied to the system (1). The error was measured using the L^{∞}-norm, defined in (3). Table 2 summarizes the relationship between the step size h, the numerical error, and the estimated convergence rate. The results demonstrate that the error decreases as $\mathfrak{h} \to 0$, with an estimated convergence rate of approximately 1.98, indicating second-order convergence. This result aligns with the theoretical expectations for the chosen discretization scheme. Furthermore, the stability of the method was verified by observing

bounded errors for sufficiently small $\mathfrak{h}$, ensuring reliable approximations of the solution.

Table 2: Convergence Analysis Results for the Caputo-Fabrizio Model

Step Size ($\mathfrak{h}$)	**Error (L^∞-norm)**	**Convergence Rate**
0.100	1.234567×10^{-2}	–
0.050	3.456789×10^{-3}	1.98
0.020	8.901234×10^{-4}	1.96
0.010	2.234567×10^{-4}	1.99

The order of the fractional derivative $\mathfrak{a}$ plays a vital role in shaping the temporal dynamics of system (1). To analyze this influence, we simulate the model for different values of $\mathfrak{a}$ and observe the resulting behaviour in each compartment, as illustrated in the following figures. Figure 6 indicates a more aggressive infection spread in systems with

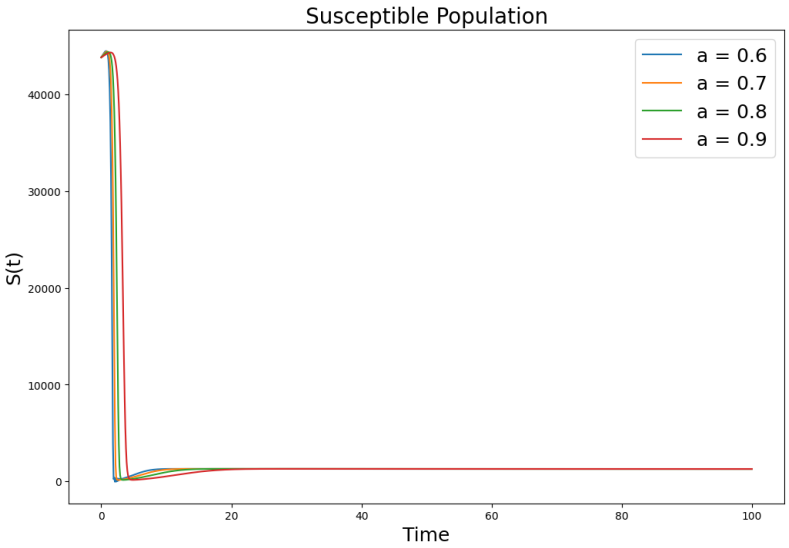

Figure 6: Susceptible class

stronger memory (i.e., lower $\mathfrak{a}$). For example, when $\mathfrak{a} = 0.6$, the susceptible population depletes sharply and rapidly compared to higher values of $\mathfrak{a}$. In Figure 7, the peak of the exposed class shifts slightly later and becomes broader as $\mathfrak{a}$ increases. This suggests that higher fractional orders slow the transition from exposed to infected class due to weaker memory effects. Figure 8 shows that the infected population peaks later and declines more gradually with increasing $\mathfrak{a}$, indicating prolonged infection periods in systems with less memory influence. As shown in Figure 9, the recovery curve flatter and shifts to the right with increasing $\mathfrak{a}$, implying delayed recovery in systems with reduced memory.

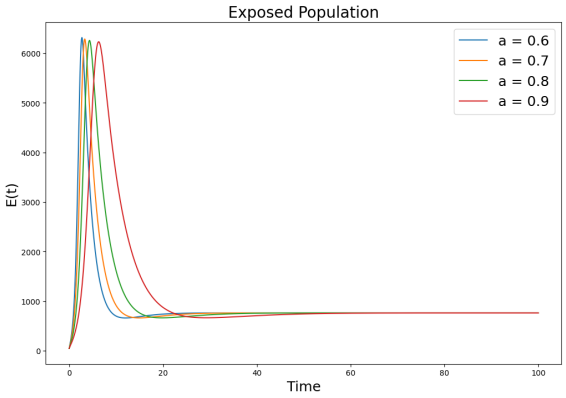

Figure 7: Exposed class

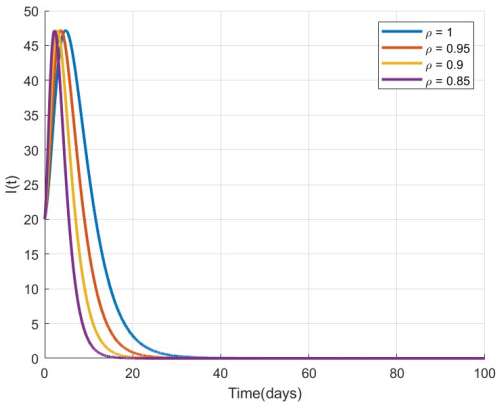

Figure 8: Infected class

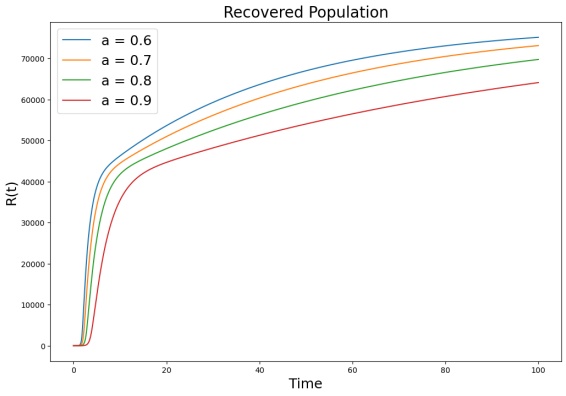

Figure 9: Recovered class

7. Conclusion

In this work, we presented a model for Lumpy skin disease within the framework of the Caputo-Fabrizio fractional derivative. Initially, we enhanced the existence theory for the

model, establishing both the existence and uniqueness of solutions through a fixed-point approach. Following the results derived, we investigated the stability of the solutions using Ulam-Hyers stability criteria. Not only this, we have also analysed the disease-free and disease-endemic equilibrium points of our proposed system. Furthermore,we conducted numerical experiments to validate the model, developing a numerical scheme that is subsequently utilized to generate graphical results. Our numerical simulations produce realistic graphs, which are thoroughly explained in the numerical section of the paper across various orders of the Caputo-Fabrizio fractional derivatives. We believe, the analysis will provide insight for formulation of policies to control the spread of LSD and thus help in achieving the UN SDG Goal-3 (health and wellness), 15(Life on land) and other related goals of [1]. We encourage readers to explore the model further using alternative numerical techniques and different fractional operators to gain deeper insights into Lumpy skin disease dynamics.

Acknowledgements

This project is sponsored by Prince Sattam Bin Abulaziz University (PSAU) as part of funding for its SDG Roadmap Research Funding Programme Project Number PSAU-2023-SDG-107.

Conflict of interest

The authors declare no conflict of interest.

References

[1] United Nations. The 17 goals. Sustainable Development Goals 1, Department of Economic and Social Affairs, United Nations, 2016.

[2] R. Alexander, W. Plowright, and D. Haig. Cytopathogenic agents associated with lumpy skin disease of cattle. *Bulletin of epizootic diseases of Africa*, 5:489–492, 1957.

[3] A. Diallo and G. J. Viljoen. Genus capripoxvirus. In A. A. Mercer, A. Schmidt, and O. Weber, editors, *Poxviruses*, pages 167–181. Birkhäuser Basel, Basel, 2007.

[4] B. Sanz-Bernardo, I. R. Haga, N. Wijesiriwardana, P. C. Hawes, J. Simpson, and et al. Lumpy skin disease is characterized by severe multifocal dermatitis with necrotizing fibrinoid vasculitis following experimental infection. *Veterinary Pathology*, 57:388–396, 2020.

[5] F. G. Davies. Lumpy skin disease, an african capripox virus disease of cattle. *British Veterinary Journal*, 147:489–503, 1991.

[6] S. Babiuk, T. R. Bowden, D. B. Boyle, D. B. Wallace, and R. P. Kitching. Capripoxviruses: an emerging worldwide threat to sheep, goats and cattle. *Transboundary and Emerging Diseases*, 55:263–272, 2008.

[7] F. G. Davies. Lumpy skin disease of cattle: a growing problem in africa and the near east. *World Animal Review*, 68:37–42, 1991.

[8] E. Young, P. A. Basson, and K. E. Weiss. Experimental infection of game animals with lumpy skin disease virus (prototype strain neethling). *Onderstepoort Journal of Veterinary Research*, 37:79–87, 1970.

[9] T. D. Dao, L. H. Tran, H. D. Nguyen, T. T. Hoang, G. H. Nguyen, and et al. Characterization of lumpy skin disease virus isolated from a giraffe in vietnam. *Transboundary and Emerging Diseases*, 69:e3268–e3272, 2022.

[10] R. Kumar, B. Godara, Y. Chander, J. P. Kachhawa, R. K. Dedar, and et al. Evidence of lumpy skin disease virus infection in camels. *Acta Tropica*, 242:7, 2023.

[11] C. M. Chihota, L. F. Rennie, R. P. Kitching, and P. S. Mellor. Mechanical transmission of lumpy skin disease virus by aedes aegypti (diptera: Culicidae). *Epidemiology and Infection*, 126:317–321, 2001.

[12] V. M. Carn and R. P. Kitching. An investigation of possible routes of transmission of lumpy skin disease virus (neethling). *Epidemiology and Infection*, 114:219–226, 1995.

[13] C. M. Chihota, L. F. Rennie, R. P. Kitching, and P. S. Mellor. Attempted mechanical transmission of lumpy skin disease virus by biting insects. *Medical and Veterinary Entomology*, 17:294–300, 2003.

[14] E. S. Tuppurainen, E. H. Venter, J. A. Coetzer, and L. Bell-Sakyi. Lumpy skin disease: attempted propagation in tick cell lines and presence of viral dna in field ticks collected from naturally-infected cattle. *Ticks and Tick-borne Diseases*, 6:134–140, 2015.

[15] S. Gubbins. Using the basic reproduction number to assess the risk of transmission of lumpy skin disease virus by biting insects. *Transboundary and Emerging Diseases*, 66:1873–1883, 2019.

[16] K. Weiss. Lumpy skin disease virus. In *Cytomegaloviruses Rinderpest Virus Lumpy Skin Disease Virus*, pages 111–131. Springer, 1968.

[17] N. Kumar and B. N. Tripathi. A serious skin virus epidemic sweeping through the indian subcontinent is a threat to the livelihood of farmers. *Virulence*, 13(1):1943–1944, Dec 2022.

[18] Department SR. Cattle population in india 2016–2023, Dec 1 2022. Statistical Report.

[19] A. A. Ali, A. N. F. Neamat-Allah, H. A. E. Sheire, and R. I. Mohamed. Prevalence, intensity, and impacts of non-cutaneous lesions of lumpy skin disease among some infected cattle flocks in nile delta governorates, egypt. *Comparative Clinical Pathology*, 30:693–700, 2021.

[20] OIE World Organisation for Animal Health. Version adopted by the world assembly of delegates of the oie in may 2010, oie, paris: Terrestrial manual of lumpy skin disease, 2010. Official document.

[21] K. MacOwan. Observations on the epizootiology of lumpy skin disease during the first year of its occurrence in kenya. *Bulletin of Epizootic Diseases of Africa*, 7:7–20, 1959.

[22] E. S. Tuppurainen and C. A. Oura. Review: lumpy skin disease: an emerging threat to europe, the middle east and asia. *Transboundary and Emerging Diseases*, 59:40–48,

2012.

[23] J. A. House, T. M. Wilson, S. E. Nakashly, I. A. Karim, I. Ismail, and et al. The isolation of lumpy skin disease virus and bovine herpesvirus-from cattle in egypt. *Journal of Veterinary Diagnostic Investigation*, 2:111–115, 1990.

[24] I. Lojkić, I. Šimić, N. Krešić, and T. Bedeković. Complete genome sequence of a lumpy skin disease virus strain isolated from the skin of a vaccinated animal. *Genome Announcements*, 6:e00482–18, 2018.

[25] N. Kumar, Y. Chander, R. Kumar, N. Khandelwal, T. Riyesh, and et al. Isolation and characterization of lumpy skin disease virus from cattle in india. *PLoS One*, 16:e0241022, 2021.

[26] F. A. Salib and A. H. Osman. Incidence of lumpy skin disease among egyptian cattle in giza governorate, egypt. *Veterinary World*, 4, 2011.

[27] S. Babiuk, T. Bowden, G. Parkyn, B. Dalman, L. Manning, and et al. Quantification of lumpy skin disease virus following experimental infection in cattle. *Transboundary and Emerging Diseases*, 55:299–307, 2008.

[28] E. M. E. Mathivanan, K. Raju, and R. Murugan. Outbreak of lumpy skin disease in india 2022 – an emerging threat to livestock and livelihoods. *Global Biosecurity*, 5, 2023.

[29] S. B. Sudhakar, N. Mishra, S. Kalaiyarasu, S. K. Jhade, D. Hemadri, and et al. Lumpy skin disease (lsd) outbreaks in cattle in odisha state, india in august 2019: Epidemiological features and molecular studies. *Transboundary and Emerging Diseases*, 67:2408–2422, 2020.

[30] P. D. Minor, A. John, M. Ferguson, and J. P. Icenogle. Antigenic and molecular evolution of the vaccine strain of type 3 poliovirus during the period of excretion by a primary vaccinee. *Journal of General Virology*, 67:693–706, 1986.

[31] K. Yasir, K. Muhammad Altaf, Fatmawati, and F. Naeem. A fractional bank competition model in caputo-fabrizio derivative through newton polynomial approach. *Alexandria Engineering Journal*, 60(1):711–718, 2021.

[32] R. Singh, A. Akgül, J. Mishra, and V. K. Gupta. Mathematical evaluation and dynamic transmissions of a cervical cancer model using a fractional operator. *Contemporary Mathematics*, 5(3):2646–2667, Jul 16 2024. [cited 2025 Mar. 31].

[33] Preety Kumari, Harendra Pal Singh, and Swarn Singh. Global stability of novel coronavirus model using fractional derivative. *Computational and Applied Mathematics*, 42(8):346, 2023.

[34] Jagdev Singh, Devendra Kumar, and Dumitru Baleanu. On the analysis of fractional diabetes model with exponential law. *Advances in Difference Equations*, 2018(1):1–15, 2018.

[35] Seher Melike Aydogan, Dumitru Baleanu, Hakimeh Mohammadi, and Shahram Rezapour. On the mathematical model of rabies by using the fractional caputo–fabrizio derivative. *Advances in Difference Equations*, 2020(1):382, 2020.

[36] Azhar Iqbal Kashif Butt. Dynamical modeling of lumpy skin disease using atangana–baleanu derivative and optimal control analysis. *Modeling Earth Systems and Environment*, 11(1):27, 2025.

[37] National Dairy Development Board. Livestock population in india by species, 2025. Accessed: 2025-03-31.

[38] K. S. Nisar, S. Ahmad, A. Ullah, K. Shah, H. Alrabaiah, and M. Arfan. Mathematical analysis of sird model of covid-19 with caputo fractional derivative based on real data. *Results in Physics*, 21:103772, 2021.

[39] M. Caputo and M. Fabrizio. A new definition of fractional derivative without singular kernel. *Progress in Fractional Differentiation and Applications*, 1:1–13, 2015.

[40] J. Losada and J. J. Nieto. Properties of a new fractional derivative without singular kernel. *Progress in Fractional Differentiation and Applications*, 1:87–92, 2015.

[41] A. A. Thirthar, H. Abboubakar, A. L. Alaoui, and K. S. Nisar. Dynamical behavior of a fractional-order epidemic model for investigating two fear effect functions. *Results in Control and Optimization*, 16:100474, 2024.

[42] K. Muthuvel, K. Kaliraj, K. S. Nisar, and V. Vijayakumar. Relative controllability for ψ-caputo fractional delay control system. *Results in Control and Optimization*, 16:100475, 2024.

[43] K. S. Nisar. A constructive numerical approach to solve the fractional modified camassa-holm equation. *Alexandria Engineering Journal*, 106:19–24, 2024.

[44] Stefan Banach. Sur les opérations dans les ensembles abstraits et leur application aux équations intégrales. *Fundamenta mathematicae*, 3(1):133–181, 1922.